

# Simulation of Neutron Irradiation Corrosion of Zr-4 Alloy Inside Water Pressure Reactors by Ion Bombardment

**X. D. Bai\*, S. G. Wang, J. Xu, H. M. Chen and Y.D. Fan**

Department of Materials Science and Engineering  
Tsinghua University, Beijing 100084, China

\*The corresponding author

Fax: 8610-62562768

E-mail: zjz-dms@mail.tsinghua.edu.cn

## **ABSTRACT**

In order to simulate the corrosion behavior of Zr-4 alloy in pressurized water reactors, it was implanted (or bombarded) with 190keV  $Zr^+$  and  $Ar^+$  ions at liquid nitrogen temperature and room temperature respectively, up to a dose of  $5 \times 10^{15} \sim 8 \times 10^{16}$  ions/cm<sup>2</sup>. The oxidation behavior and electrochemical behavior were studied on implanted and unimplanted samples. The oxidation kinetics of the experimental samples were measured in pure oxygen at 923K and 133.3Pa. The corrosion parameters were measured by anodic polarization methods using a Princeton Applied Research Model 350 corrosion measurement system. Auger Electron Spectroscopy (AES) and X-ray Photoelectric Spectroscopy (XPS) were employed to investigate the distribution and the ion valence of oxygen and zirconium ions inside the oxide films before and after implantation. It was found that: 1) the  $Zr^+$  ion implantation (or bombardment) enhanced the oxidation of Zircaloy-4 and resulted in that the oxidation weight gain of the samples at a dose of  $8 \times 10^{16}$  ions/cm<sup>2</sup> was 4 times greater than that of the unimplantation ones; 2) the valence of zirconium ion in the oxide films was classified as  $Zr^0$ ,  $Zr^+$ ,  $Zr^{2+}$ ,  $Zr^{3+}$  and  $Zr^{4+}$  and the higher valence of zirconium ion increased after the bombardment; 3) the anodic passivation current density is about 2 ~ 3 times that of the unimplanted samples; 4) the implantation damage function of the effect of ion implantation on corrosion resistance of Zr-4 alloy was established.

## 1. INTRODUCTION

There exist similarities and correlation between the damage or defects in materials generated by ion bombardment and by neutron irradiation. Simulations of changes in properties of material induced by neutron irradiation have been done with using ion bombardment since early 1960's[1], mainly on mechanical properties of nuclear materials. Less attention, on the other hand, has been paid to their corrosion behavior. Furthermore, no authentic systematic comments or theories on this subject had appeared until the Sikeborgh meeting in 1990[2].

In the meeting, ion bombardment method was proved to have many advantages; those are: 1) much higher displacement rate leading to a shorter irradiation duration; 2) little nuclear reactions; 3) precise control of bombardment conditions; 4) a lower irradiation cost than that of neutron irradiation.

It is believed that the smaller the effects of implanted ions on the properties of the substrate materials are, the better simulation experiment is. So, two kinds of ions are taken into account. 1) Self-ions are the best for simulating the damage process induced by neutron irradiation, because they do not induce the sub-alloy process and are favorable to create the pure damage process in the target materials. Zircaloy-4 contains Sn: 1.4 wt%, Fe: 0.23 wt%, Cr: 0.1 wt% and Zr as balance component. Then, the best self-ion for this alloy should be Zr ion. Furthermore, a small amount of ions of Sn, Fe and Cr (great lower than their content in the alloy) should also be regarded as self-ions under the condition that their bombardment should not cause sub-alloy process. 2) Ions of inert gas can also be used to create the pure damage process, yet, with a disadvantage of the formation of gas bubbles in target materials when their dose is high.

It is believed that the corrosion mechanism of Zircalloys in Pressureized Water Reactors (PWR) proceeds mainly through the oxidation process and electrochemical corrosion process. So, in this study, the corrosion behavior of Zircaloy-4 under neutron irradiation is simulated by  $Zr^+$  bombardment, then the subsequent oxidation was done in oxygen pressure of 133.3 Pa at 923K, and the effect of ion implantation damage on the polarization behavior of Zircaloy-4 was investigated with the potentiokinetic technique in 1N  $H_2SO_4$  at room temperature. After experiments, the irradiation enhancement of oxidation of Zircaloy-4 is described. Then, the oxygen concentration and the ion valence distribution inside the oxide films are presented with the effect of  $Zr^+$  ion bombardment. Finally an oxidation mechanism in terms of the effect of irradiation enhancement of the electric field of space charge across the oxide films is proposed.

## 2. EXPERIMENT

Samples were machined to 10mm×10mm×1.5mm from a sheet of Zircaloy-4, completely recrystallized by vacuum annealing. The composition of the alloy is shown in Table 1.

Table 1: Composition of Zr-4 alloy

Element	content(wt%)
Zr	bal
Sn	1.4%
Fe	0.23%
Cr	0.1%
Ni	60ppm
Al	<14ppm
Ti	<14ppm
Co	<14ppm
Mn	<14ppm
Mg	<14ppm
Pb	<14ppm
W	<14ppm
Mo	<20ppm
Cu	<20ppm
Si	<50ppm
Cl	<20ppm
C	<100ppm
N	<30ppm
O	<900ppm
H	<10ppm
Hf	<100ppm
B	<0.5ppm
Cd	<0.5ppm

The samples were abraded with sand paper of 300, 500 and 800 grit of SiC, degreased in acetone and ethanol, chemically polished in the solution of 10% HF, 30% HNO<sub>3</sub> and 60% H<sub>2</sub>O in volume, rinsed in natural water more than 3 times and finally rinsed in deionized water.

## 2.1 Oxidation experiment

The samples were slightly oxidized in advance within an autoclave filled with water at  $7.20 \times 10^4$  Pa and 673K for different duration. The thickness of films was determined to be 6nm, 18nm, 28nm and 75nm using Rutherford Back Scattering (RBS).

Bombardments were performed with 190 keV  $Zr^+$  ions at a dose rate of  $9.65 \times 10^{12}$  ions/cm<sup>2</sup> to doses of  $5 \times 10^{15}$ ,  $5 \times 10^{16}$  and  $8 \times 10^{16}$  ions/cm<sup>2</sup>, at liquid nitrogen temperature in a vacuum pressure of better than  $1.33 \times 10^{-3}$  Pa.

The oxidation was carried out with a hot oxidation balance with an accuracy of  $10^{-6}$  gram. For oxidation, firstly, the sample of Zircaloy-4 was hung up with a platinum wire of 0.2 mm in diameter in a vacuum chamber, then the high purity (99.93%) Ar gas was introduced into the chamber to protect the sample from serious oxidation during heating. When temperature reached 923K, Ar gas was turned off and oxygen gas of 99.98% purity was introduced at once up to its final partial pressure 133.3Pa within 20 seconds, and the sample was oxidized for 5 minutes. The weight data curve was recorded all the time.

## 2.2 Electrochemical experiment

$Ar^+$  ions bombardment was conducted using 190kV ion accelerator at room temperature, and the fluence were  $5 \times 10^{14}$  ions/cm<sup>2</sup> and  $2.5 \times 10^{15}$  ions/cm<sup>2</sup> respectively. In order to prevent the surface of Zr-4 from oxidizing, Zr-4 samples worked in  $10^{-3}$  Pa vacuum.

Potentiodynamic tests carried out in 1N H<sub>2</sub>SO<sub>4</sub> using a Princeton Applied Research Model 350 corrosion measurement system at room temperature. Each of test samples had a 1cm<sup>2</sup> area for the working electrode. The scan rate was 2.0mV/s. All potential measurements were taken with respect to a saturated calomel electrode (SCE). Immediately after samples immersed in the solution, a anodic scan was done starting in cathodic region (approximately -1.0V with respect to the SCE) and scanning into the anodic region to approximately +2.0V with respect to the SCE.

## 2.3 Analysis

Auger Electron Spectroscopy (AES) analysis was conducted with use of a Perkin Elmer PHI-60 spectrometer to obtain the distribution of oxygen ions in the oxide films of Zircaloy-4 before and after bombardment with  $Zr^+$  ions.

X-Ray Photoelectronic Spectroscopy (XPS) was also measured by using a Kratos XSAM 800 spectrometer to analyze the distribution of the valence of zirconium and oxygen ions as a function of the depth of oxide films. The samples were excited by Al-K $\alpha$  X-ray of 1.4866keV and their surfaces were sputtered by keV  $Ar^+$  ions. The scanning range for the Zr-3d and the O-1s spectroscopy was 20 and 15eV, respectively. A DS300X

data processing system was used to analyze the spectra.

A computer program TRIM-92 was adopted to calculate the depth dependence of damage level in the unit of displacement per atom (dpa).

### 3. RESULTS AND DISCUSSION

#### 3.1 Oxidation experiment

##### 3.1.1 Influence of $Zr^+$ ion bombardment on oxidation behavior of Zircaloy-4 with a original oxide film of 6nm thick

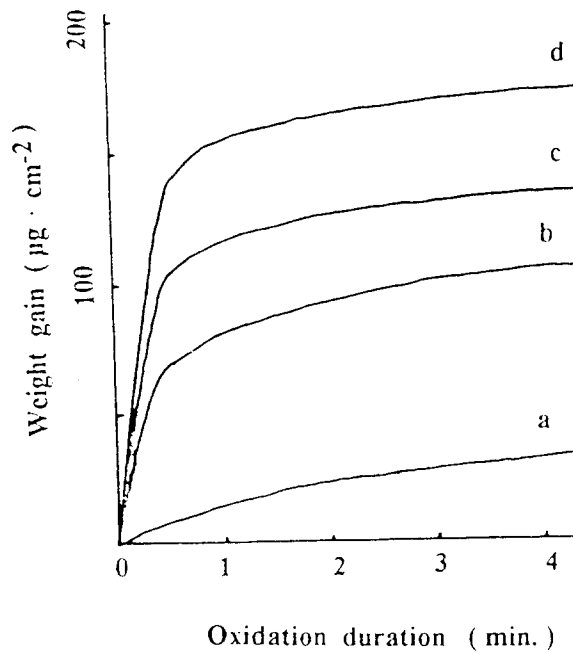


Fig. 1 Influence of  $Zr^+$  bombardment on oxidation of Zircaloy-4 with a original oxide film of 6nm thick, a: unbombarded, b, c and d: bombarded with doses of  $5 \times 10^{15}$ ,  $5 \times 10^{16}$ , and  $8 \times 10^{16}$  ions/cm<sup>2</sup> respectively.

Table 2. The relationship between dpa inside the oxide film and oxidation weight gain, where  $w_0$  and  $w_i$  are weight gains under zero dose and under bombardment with dose i.

dose(ions/cm <sup>2</sup> )	dpa	w( $\times 10^{-6}$ g)	$w_i/w_0$
0	0	34	1
$5 \times 10^{15}$	10.7	106	3.12
$5 \times 10^{16}$	107	134	3.94
$8 \times 10^{16}$	71.2	172	5.06

As shown in Fig. 1 and Table 2, the oxidation weight gain increases as increasing oxidation time, with the higher rate for the higher  $Zr^+$  ion dose and the oxidation rate of specimens bombarded to the dose of  $8 \times 10^{16}$  ions/cm<sup>2</sup> was 4 times larger than that of unbombarded samples.

Hillner and Asher et al.[3~5] reported that the neutron irradiation enhanced the oxidation of Zircaloy-2 and Zircaloy-4 under the operating condition of PWR and that the oxidation weight gain increased up to 2~4 and 10 times greater than that of the unirradiated ones for Zircaloy-2 and Zircaloy-4 under a neutron flux of  $4 \times 10^{13}$  n/cm<sup>2</sup>/s (energy greater than 1MeV). These values are very close to those obtained under  $Zr^+$  ion bombardment in the present result as well. This suggests that the corrosion of Zircaloy-4 under neutron irradiation can be simulated by ion bombardment.

### 3.1.2 The relationship between dpa and weight gain

Many authors have reported [6~8] that under neutron irradiation or ion bombardment, the decomposition of  $Zr(Fe,Cr)_2$  precipitates takes place to form Fe depleted torus zones around them due to diffusion of Fe atoms into the matrix, and that the corrosion resistance of Zircaloy-4 becomes worse due to the Fe depleted zones. It has also been reported[9] that the width of the Fe depleted zone is proportion to the 0.45th power of the ion dose. The oxidation weight gain is shown in Table 1 as a function of dpa inside the oxide films. On the basis of the previous[10] and the present results, the fractional weight  $w_i/w_0$  is correlated with dpa as

$$w_i/w_0 = 1.664 + 0.590 \ln(\text{dpa}) \quad (1)$$

with the correlation coefficient  $r=0.899$ , where  $w_0$  and  $w_i$  are weight gains under zero dose and under bombardment with dose  $i$ .

### 3.1.3 The damage function of irradiation corrosion

Traditionally, the dpa has been used as unit to describe the irradiation damage in materials, however it is not an exact parameter for depicting the irradiation corrosion. Since most displaced atoms disappear through the mutual recombination and/or diffusion into the grain boundaries, it is believed that they play no significant role in the corrosion process.

We define the irradiation corrosion damage function,  $G(E)$  and express the weight gain increment caused by ion bombardment,  $\Delta W$ , by using the follow equation[11]

$$\Delta W = \int_{E_{\min}}^{E_{\max}} D \cdot G(E) \cdot \psi(E) dE / \int_{E_{\min}}^{E_{\max}} \psi(E) dE \quad (2)$$

where D is the ion dose, G(E) the damage function,  $\psi(E)$  the ion energy distribution function of incident ions which ranges from  $E_{\min}$  to  $E_{\max}$  and E ion energy. When a monoenergetic ion beam is used as being done in this experiment, Eq.(2) can be simplified as:

$$\Delta W = D \cdot G \quad (3)$$

Based on the data in Table 2 and Eq.(3), the damage function G was calculated as shown in Table 3 and the regression formula can be expressed as

$$\log G = -0.440(\log D)^{1.245} \quad (4)$$

with a correlation coefficient  $r=0.9969$ .

Table 3. The relation between  $Zr^+$  ion dose and damage function G

D(ion/cm <sup>2</sup> )	G=W/D(g/ion)
$5 \times 10^{15}$	$1.44 \times 10^{-14}$
$5 \times 10^{16}$	$2.00 \times 10^{-15}$
$8 \times 10^{16}$	$2.76 \times 10^{-15}$

### 3.1.4 The influence of $Zr^+$ bombardment on the ionic valence of the oxide films of Zircaloy-4 and the mechanism of the enhanced oxidation by ion bombardment

Fig. 2 gives the ion valences and their change inside the oxide films of 75nm before and after  $Zr^+$  ion bombardment. Eloff et al.[12] have described that there exists an electric field of space charge across the oxide film which promotes the movement of electrons and the ion diffusion to enhance the oxidation.

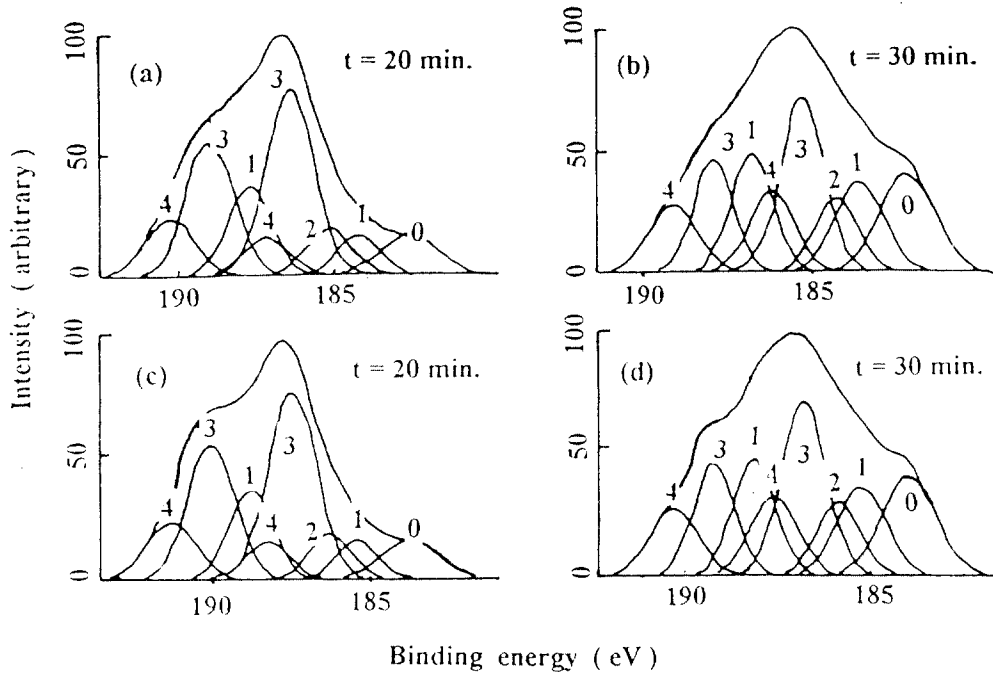


Fig. 2 The distribution of  $Zr^{i+}$  ( $i=0, 1, 2, 3,$  and  $4$ ) ion valences inside the oxide films of 75nm thick before and after  $Zr^+$  ion bombardment. (a) and (b): Zircaloy-4 before bombardment, (c) and (d): after bombardment,  $t$ : sputtering time with keV  $Ar^+$  ions. 0, 1, 2, 3, and 4 correspond to  $Zr^0, Zr^{1+}, Zr^{2+}, Zr^{3+},$  and  $Zr^{4+}$  ions, respectively.

It can be found in Fig. 2 that there exist distributions of Zr ions with different valences; that is higher (+4) valence at the surface zone and the lower (0) ones inside the matrix both in the unbombarded and bombarded oxide films. It is generally accepted that the oxidation of Zircaloy-4 proceeds through inward diffusion of oxygen atoms based on the vacancy diffusion mechanism. That is, at the surface oxide film, the oxygen atoms obtain electrons from the oxide film and turn themselves into oxygen ions and go into the lattice of oxides. Whereas, at the interface between Zircaloy-4 and oxide, Zr atoms lose their electrons, turn themselves into Zr ions and react with oxygen ions resulting the oxide film. Due to the successive increase of Zr ions near the interface between Zircaloy-4 and the oxide and due to the slow diffusion of oxygen, a certain amount of oxygen vacancies might be introduced inside the oxides to meet the requirement of the electric charge balance. And then, since the diffusion of oxygen vacancies toward the surface is slower than that of electrons toward to the surface, the concentration of oxygen vacancies near the surface of oxide films is much lower than that inside, whereas the concentration of higher valence Zr ions is higher near the surface than that inside the oxide film, which build up a space charge field in the direction from the surface to the matrix across the



whole oxide film, promoting diffusion of the electrons, and therefore, enhancing the oxidation process.

Furthermore, because that the reaction of oxidation of Zirconium is a heat releasing reaction, the heat produced inside oxide film will excite and introduce more vacancies to enhance the oxidation itself.

The electronic energy state of Zirconium oxides is in the valence band of it. But Zr ion implantation creates many atomic disorder along ion tracks, and creates a certain quantity of electronic energy states distribution between the conduction and the valence bands to promote the electronic conductivity of the oxide[13] and the successive oxidation.

### 3.1.5 The surface mixture effect of oxygen with the matrix by bombardment

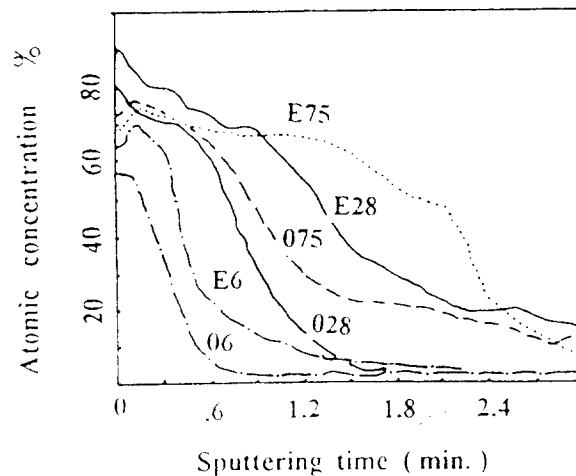


Fig. 3 The distribution of oxygen atoms in the oxide film and the matrix before and after bombardment with  $Zr^+$  ions. Sputtering time corresponds to the depth from the surface. 0 and E mean before and after bombardment respectively, and 6, 28 and 75 represent the thickness of oxide films in manometer.

As shown in Fig. 3, the oxide film becomes remarkably thicker after the bombardment with  $Zr^+$  ions. Mordant[14] found a monolayer of absorbed oxygen atoms

on the surface of samples even under a low pressure of  $1.33 \times 10^{-6}$  Pa. It is obvious that the bombardment of  $Zr^+$  ions drives the oxygen atoms into the oxide film and makes the oxide film thicker.

### 3.1.6 The effects of Ar ion sputtering on the experimental results

There existed Ar ion sputtering processes in the XPS and AES measurements. Malherbe et al.[15] investigated the preferential sputtering of the different ions on the oxides and pointed out two important actors influencing on them. One is the atomic mass effect of sputtering; the lighter the atomic masses, its sputtering yield becomes the more. Therefore oxygen atoms are more dominantly sputtered away under our experimental condition, concentration of oxygen ions shown in Fig. 3 might be lower than it actually is. Other one is the bonding energy between metallic ions and oxygen i.e. the bigger the bonding energy, the harder the oxygen can be sputtered. So that the content of the higher valance of Zr ions shown in Fig.2 is lower than it actually is, because the bonding energy of  $Zr^{4+}$ -O is 7.89eV and that of  $Zr^+$ -O is only 2.86eV. This factor supports further the characteristics of the distribution of the different valance ions inside the oxide films.

### 3.1.7 The effect of thermal diffusion on the defect distribution and on the oxidation

The primary defects created during the ion implantation is mainly vacancies and interstitial atoms. Gyulai et al.[16] found that at the end of the track of the single ion, there existed a highly disorder zone. Helllen et al.[17] pointed out that under thermal diffusion, two single vacancies could combine to form divacancy. Jones et al.[18] observed the interaction of the defects over the temperatures of 923 ~ 1023K, and found that the density of point defects decreased and that of the dislocations gradually increased.

The higher the dose, the higher the defect density and the higher the dislocation density is. Dislocations provide the easier diffusion paths for oxygen atoms and vacancies[19]. Therefore, at the higher the implantation dose, the higher the oxidation weight gain is expected.

### 3.1.8 The effect of activation energy on the oxidation under the condition of the bombardment by $Zr^+$ ions

It is believed that the weight gain of zircaloy-4 alloy in oxidation experiment can be described as equation (5):

$$\Delta W = K \cdot t^n \quad (5)$$

where  $\Delta W$  is weight gain,  $K$  is oxidation rate constant,  $t$  is oxidation time. According to Arrhenius equation, shown as

$$K = A \exp(-Q/RT) \quad (6)$$

in which  $A$ ,  $R$  are two constants,  $Q$  is activation energy,  $T$  is absolute temperature, the relationship between  $\Delta W$  and  $t$  can be expressed by equation (7):

$$\Delta W = A \exp(-Q/RT) \cdot t^n \quad (7)$$

The ability of oxidation can be expressed by activation energy ( $Q$ ). If  $Q$  is small, the oxidation will carry out smoothly. On the contrary, if  $Q$  is very large, the oxidation should be very difficult.

Under the condition of ions bombarding the zircaloy-4 alloy, high energy implanting ions bring matrix extra energy, that makes the average energy increase and close to the top of the barrier, of course, the activation energy ( $Q$ ) becomes smaller. That is the reason why bombardment can accelerate the oxidation rate.

In summary, the enhancement of oxidation after ion bombardment is attributed to the increment of defects which provide higher chemical oxidation potential and easier diffusion paths for the oxygen vacancies. The bombardment of ions creates higher valences of Zr ions near the surface zone of oxide films and forms a electric field with a direction from surface to matrix. This field will enhance the movement of the electrons toward the oxide surface and finally enhances the successive oxidation. It is deduced that in the operation condition of pressurized water reactors, if the neutron irradiation creates higher valences of Zr ions near the surface zone of the oxide film, the oxidation could be accelerated.

### 3.2 Electrochemical experiment

Irradiation enhance corrosion has been found not only in oxidation experiment, but also in electrochemical experiment. The anodic polarization curves of various fluence of  $Ar^+$  ions irradiating Zr-4 samples at room temperature are given in Fig. 4.

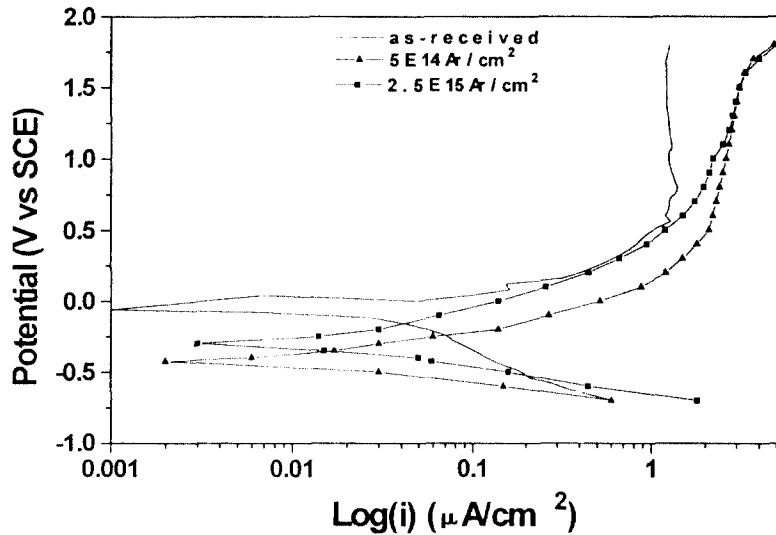


Fig. 4. Anodic polarization curves of  $\text{Ar}^+$  ions irradiating Zr-4 with the implanting dose of 0,  $5 \times 10^{14}$  and  $2.5 \times 10^{15}$  ions/cm<sup>2</sup> respectively at room temperature.

From Fig. 4. it can be found that corrosion resistance of zircaloy-4 sample implanted by  $5 \times 10^{14}$  ions/cm<sup>2</sup> or  $2.5 \times 10^{15}$  ions/cm<sup>2</sup>  $\text{Ar}^+$  ions is worse than that of as-received Zr-4 sample. The anodic passivation current density is about 2 ~ 3 times larger than that of the unimplanted sample. These values are very close to those obtained under  $\text{Zr}^+$  ion bombardment in the present result as well.

As we know, ion beam bombarding always brings all kinds of defects, such as point defects, dislocation loops, caves, to the surface of the materials. The existence of defects will damage the microstructure and change the properties. Considering the corrosion behavior, low fluence irradiation can induce many sorts of defects which always act as active corrosion points, and increase the surface heterogeneity and surface atoms activity. All these facts accelerate corrosion rate. This is the reason why low fluence of ion beam irradiation can decrease the corrosion resistance.

#### 4. CONCLUSIONS

1. Ion bombardment enhances the oxidation of Zircaloy-4 in pure oxygen at 923K and  $133 \times 10^2$  Pa, and the oxidation weight gain after bombardment of a dose of  $8 \times 10^{16}$  ions/cm<sup>2</sup> is 4 times greater than that of the unbombarded specimens.

2. The valences of Zr ions in the bombarded oxide film are detected to be  $\text{Zr}^0$ ,  $\text{Zr}^{1+}$ ,  $\text{Zr}^{2+}$ ,  $\text{Zr}^{3+}$  and  $\text{Zr}^{4+}$  and the higher valences of Zr ions are more dominant near the surface

of oxide film.

3. The regression formula of the oxidation weight gain (W) versus dpa under irradiation is expressed as  $w_i/w_0=1.664+0.590\ln(\text{dpa})$ .

4. Ion bombardment enhances the electrochemical corrosion of Zircaloy-4 in 1N H<sub>2</sub>SO<sub>4</sub> at room temperature, and the passive current density after bombardment of a dose of  $5\times 10^{14}$  ions/cm<sup>2</sup> or  $2.5\times 10^{15}$  ions/cm<sup>2</sup> is 2 ~ 3 times greater than that of the unbombarded specimens.

5. Zr<sup>+</sup> ion bombardment is effective only in proper ranges of parameters for simulating the corrosion behavior of Zircaloy-4 under neutron irradiation in PWR.

### ACKNOWLEDGMENTS

The authors would like to thank You Y J, Zhen R Y, et al. for their precious helps. We would also like to thank Analysis Center of Tsinghua University for financial support.

### REFERENCES

- [1] A.B. Adamson, in: Zirconium in Nuclear Industry, ASTM STP 551(1974), 215-7.
- [2] C. A. English, W. V. Green, N. Guinan, A. Horsewell S. Ishino, B. N. Singh and M. Victoria, J. Nucl. Mater. 174(1990), 352-4.
- [3] E. Hillner, in: Zirconium in Nuclear Industry, ASTM STP 551(1974), 449-62.
- [4] E. Hillner, in: Zirconium in Nuclear Industry, ASTM STP 551(1974), 211-35.
- [5] R. C. Asher, Corr. Sci. 10(1970), 695-707.
- [6] Anon, Electr. Power Res. Inst. Rep. USA, EPRI-NP-5591, 1988.
- [7] D. Pecheur, F. Lefebvre and C. Leimaignan, J. Nucl. Mater. 189(3), (1992), 318-32.
- [8] F. Lefebvre and C. Lemaignan, J. Nucl. Mater. 165(2), (1989), 122-7.
- [9] Y. Etoh and S. Shimada, J. Nucl. Mater. 200(1)(1993), 59-69.
- [10] R. A. Herring, J. Nucl. Mater., 159 (1988), 386-96.
- [11] D.R. Olander, Fundamental Aspects of Nuclear Reactor Fuel Elements, 1976, translated by H. D. Li et al, nuclear Energy Press (China), Beijing 1984, Chinese ed. pp.43.
- [12] G. A. Eloff and C. J. Greyling, J. Nucl. Mater. 199(1993), 285-8.
- [13] B. B. Ling, Principle of Engg. of Nucl. Reactors (2nd ed., in Chinese), 1989,6, Beijing, pp.46.
- [14] C. Mordant, Surf. Sci. 219(1989),331-45
- [15] J. B. Malherbe, S. Hofmann and J. M. Sanz, Applied Surf. Sci., 27 (1986), 355-65.
- [16] J. Gyulai, F.Paszti and E.Szilagyi, Nucl. Instrum. Methods in Phy. Res. B106(1-4), 328-32.

- [17] A. Hellen, P. Hakansson, N. Kesitalo, J. Olsson, A. Brunelle, S. Della-Negra, and Y. L. Beyec, Nucl. Instrum. Methods in Phy. Res. B106(1-4), 233-6.
- [18] K. S. Jones, J. Liu, L. Zhang, V. Krishnamoorthy and R. T. Dehoff, Nucl. Instrum. Mehods in Phy. Res. B106(1-4), 227-32.
- [19] H. M. Chen, X. D. Bai and C. L. Ma, Corrosion and Protection of Materials of Nuclear Reactions, Atomic Energy Press, Beijing, 1986. pp. 206.